

31

32 **Abstract**

33 Pathways of transmission of coronavirus (COVID-19) disease in the human population are
34 still emerging. However, empirical observations suggest that dense human settlements are the
35 most adversely impacted, corroborating a broad consensus that human-to-human transmission
36 is a key mechanism for the rapid spread of this disease. Here, using logistic regression
37 techniques, estimates of threshold levels of population density were computed corresponding
38 to the incidence in the human population. Regions with population densities greater than
39 3000 person per square mile in the United States have about 95% likelihood to get infected
40 with COVID-19. Since case numbers of COVID-19 dynamically changed each day until
41 November 30, 2020, ca. 4% of US counties were at 50% or higher risk of COVID-19
42 transmission. While threshold on population density is not the sole indicator for
43 predictability of coronavirus in human population, yet it is one of the key variables on
44 understanding and rethinking human settlement in urban landscapes.

45

46 **Plane language Summary:** Population density is certainly one of the key factors influencing
47 the transmission of infectious diseases like COVID-19. It is approximated that in continental
48 United States, population density of 1192 per square mile and higher presents 50%
49 probability of getting infected with COVID-19.

50

51 **Keywords:** threshold, population density, logistic regression, COVID-19.

52

53

54

55

56

57 **1.Introduction**

58 Severe Acute Respiratory Syndrome caused by Coronavirus (SARS-CoV-2 thereafter) is a
59 respiratory lung infection, and as of April 28, 2021, there have been more than 148 million
60 (WHO COVID-19 Dashboard, <https://covid19.who.int/>) confirmed human cases in the
61 world. The SARS-CoV-2 virus remains highly infectious and is circulating in the human
62 population at an alarming rate with anticipated variants in near future. An emerging
63 disciplinary consensus is that seasonal variation may lead to cyclical outbreaks in the human
64 population(Carlson, Gomez, Bansal, & Ryan, 2020; Merow & Urban, 2020). As with all
65 airborne respiratory infectious diseases, the transmission of SARS-CoV-2 is high in densely
66 populated urban regions of the world (Cruickshank, 1939; Robinson, Stilianakis, &
67 Drossinos, 2012). However, thresholds of population density relative to the outbreak of the
68 disease in humans remains unknown. The relative importance of knowledge of threshold on
69 population density with reference to infectious disease such as COVID-19 is important for
70 the future of modern cities and urban landscapes in the USA, given about 71% of the
71 population reside in urbanized areas with an average density of 2534 persons per square mile
72 ([https://www.census.gov/programs-surveys/geography/guidance/geo-areas/urban-rural/ua-](https://www.census.gov/programs-surveys/geography/guidance/geo-areas/urban-rural/ua-facts.html)
73 [facts.html](https://www.census.gov/programs-surveys/geography/guidance/geo-areas/urban-rural/ua-facts.html)).

74 Influenza transmission dynamics, which allow parallel comparison with COVID-19
75 transmission, depend on several socio-demographic factors (such as race, income level,
76 education, and location), but population density remains a critical variable for controlling
77 an outbreak of seasonal influenza (Atkinson & Wein, 2008; Merler & Ajelli, 2010). While
78 the severity of airborne contagion cannot be attributed solely to population density(Li,
79 Richmond, & Roehner, 2018), the knowledge of thresholds on population density can
80 be helpful in understanding the spatial distribution with respect to the risk

81 of disease(Chandra, Kassens-Noor, Kuljanin, & Vertalka, 2013; Grantz et al., 2016).
82 Intuitively, high population density is concluded to favor contagion and vice-versa. However,
83 non-uniform distribution of a population can yield inconclusive results (Li et al., 2018).
84 While the significant association was reported between population density and
85 transmissibility for the 1918 influenza pandemic in Chicago (Grantz et al., 2016), the average
86 influenza attack rates decreased with increasing population density in Japan (Hoyle &
87 Wickramasinghe, 1990). In the context of COVID-19, an analysis of Brazilian data
88 suggests the general increase in COVID-19 cases was associated with highly populated
89 regions(Pequeno et al., 2020). There is no study to date that provides an exploratory
90 association of population density thresholds with COVID-19 cases in the continental USA.

91 This study was undertaken to determine thresholds on population density that can be used to
92 estimate the probable risk of infection from COVID-19. Estimation of a threshold
93 population density would allow in the differentiation of low and high-risk regions and offer
94 useful input for planning, designing, and targeting public health interventions. Also,
95 identifying specific regions where greater surveillance is required to contain the disease
96 would be enhanced and can be used to define the expansion of urbanized areas in the USA.

97 **2. Methods**

98 Daily incidence data for COVID-19 cases in the 3,107 mainland U.S. counties were obtained
99 from the GitHub project (<https://github.com/nytimes/covid-19-data>) from March 15, 2020, to
100 November 30, 2020. The time period was selected based on the non-availability of vaccines
101 since vaccines will mask the limit on population densities. Data on the population densities
102 of each U.S. county were obtained from the U.S. Census Bureau (2019)
103 (<https://www.census.gov/data/datasets/time-series/demo/popest/2010s-counties-total.html>).
104 Land area in square miles was obtained from the U.S. Census Bureau
105 (<https://www.census.gov/library/publications/2011/compendia/usa-counties->

2011.html#LND). An ordinal logistic regression model was employed to study the dependency of COVID-19 cases (thereafter cases) on counties' population density. It was assumed that the population densities remained constant during the study period, implying population mobility has minimal impact on population density. Further, the population was assumed to be uniformly distributed over the county. Since the number of cases differs widely over the county, intuitively, it is preferable to classify cases into a number of classes where each class explicitly implies a specific infection risk. To classify cases, we estimated the percentile of cumulative cases at an interval of 15 days beginning March 15, 2020, to November 30, 2020. Cumulative cases data were divided into three categories (or events): (a) low number of cases (up to 80th percentile); (b) medium number of cases (80th to 95th percentile); and (c) high number of cases (greater than 95th percentile). The 80th percentile case on November 30, 2020 was 3817 (Table 1), which can still be considered relatively less compared to the number of cases in high-risk locations.

Table 1: Biweekly 80th percentile cases of low cases

Date	80th percentile cases
March 15 2020	0
March 31 2020	15
April 15 2020	63
April 30 2020	126
May 15 2020	196
May 31 2020	271
June 15 2020	351
June 30 2020	480
July 15 2020	670
July 31 2020	970
August 15 2020	1175
August 31 2020	1382
September 14 2020	1564
September 30 2020	1787
October 15 2020	2069
October 31 2020	2410
November 15 2020	3036
November 30 2020	3817

121 Moreover, a higher value for the log-likelihood (a statistical metric used for model selection)
122 in Table 2, justifies the choice of the 80th percentile. In fact, the log-likelihood function was
123 found to be better with increasing percentile, with the increase being less for the percentiles
124 above the value of 80.

125 **Table 2:** Variation in log-likelihood in COVID-19 cases

Percentile up to which cases were considered low	log likelihood
33	-3070.07
50	-2860.07
80	-1634.02
85	-1364.49

126 Thus, the ‘reasonable’ choice of percentiles for classification of cases will lead to overall
127 similar model results without altering the final interpretation.. The following paragraph
128 briefly explains the analysis approach. Relevant theory for the application of ordinal logistic
129 regression is detailed in the supplementary section.

130 The predictor used is the county population density which is the county's population per unit
131 of the county's land area. The response variable, which is ordinal in nature, is the cumulative
132 case count classified into low, medium, and high (based on percentiles). Logit link function
133 (details in supplementary section) was used to express the dependent variable as a linear
134 function of the independent variables. Link function also relates the response (ordinal cases)
135 to linear predictor (population density) and transforms the probabilities of ordinal response to
136 the continuous scale [0,1]. The regression equations, thus, take the form as follows:

137
$$\ln \left(\frac{p(\text{high cases})}{1-p(\text{high cases})} \right) = \alpha_1 + \beta * \text{population density} [1]$$

138
$$\ln \left(\frac{p(\text{medium cases})}{1-p(\text{medium cases})} \right) = \alpha_2 + \beta * \text{population density} [2]$$

139

140 where $p(\text{high cases})$ and $p(\text{medium cases})$ are the probabilities of high and medium cases,
141 respectively. Constants and coefficients in the equations (1, 2) were estimated using the
142 maximum likelihood estimation methods. Since the total probabilities sum up to one, the
143 probability of a low number of cases were estimated by subtracting the probability of high
144 and medium cases.

145 **3. Results and discussion**

146 We start our analysis with results obtained from logistical regression models (Figure 1)
147 showing three critical statistical metrics (Somers D, Goodman-Kruskal Gamma and Percent
148 Concordant pairs).

149

150

151 High values of measures of association ($> 82\%$), i.e., percentage of concordant pairs,
152 Somers's D and Goodman-Kruskal Gamma, signify that the performance of ordinal logistic
153 model is satisfactorily. On average, model performance remained constant since start of
154 collection of data on COVID-19 human cases. The p-values for each constant and predictor
155 population density were less than 0.05 (not shown), thus establishing statistical significance.
156 The p-value for the test of all slopes is zero (Table S1), which indicates the predictor
157 population density has a statistically significant relationship with the response variable
158 (COVID-19 cases). The deviance goodness of fit result ($p>0.05$), for all dates for which the
159 model was run, showed adequate fit for the data, and the associated probabilities do not
160 deviate significantly from observed values (detailed inference of model performance
161 indicators for November 15, 2020 is presented in Table S1 in supplementary section). The
162 model results for any one day should sufficiently explain the behavior of event probability
163 (cases) with population density. The plots in Figure 2 show average probability of high,
164 medium, and low number of cases.

165

166

167 Average probabilities were defined as the mean of the probabilities obtained from the ordinal
168 logistic regression models for each of the eighteen bi-weekly cases (from March 15, 2020, to
169 November 30, 2020). The monotonic nature of Figure 2(a) shows that with an increasing
170 population density, the probability of a high number of cases increases, and vice versa. The
171 probability rises steeply to a nearly constant value of 1 at a population density of ca. 5000 per
172 square mile, suggesting larger population densities greater than this value were remarkably
173 associated with the corresponding high number of COVID-19 cases. The implication is that
174 the pronounced effect of high population density and a proportional number of cases was
175 sufficient to establish population density as an important factor in transmission potential of
176 this disease . The results suggest that in densely populated areas, it may be challenging to
177 follow social distancing norms, thus an increased number of COVID-19 human cases were to
178 be expected. Figure 2(c) shows the probability of a low number of cases, a trend opposite to
179 that for high number of cases. The probability continuously decreases to a constant value
180 close to zero, signifying that as population density increases, the chance of a low number of
181 cases decreases. Figure 2(b) illustrates the medium number of cases with population density.
182 The maximum probability of the medium number of cases is ca. 0.48, corresponding to the
183 population density of ca. 1,190 per square mile. Thus, a decrease in population density from
184 1,190 per square mile decreases the probability of a medium number of cases as the
185 probability of low number of cases increase. On the other hand, if population density beyond
186 1,190 per square mile, the probability for a medium number of cases decreases since
187 probability of high number of cases increase thereafter. Population density of 1,190 people
188 per square mile can be interpreted as a transition from low to high COVID-19 cases. Figure 3
189 illustrates changes in event probabilities over time and suggests that even low-density

190 counties are likely to be more vulnerable as the probability of high number of COVID-19
191 cases for population density increases over time.

192

193 In Figure 2(a), the threshold population density is shown at which a 50% chance of a high
194 number of cases will occur, ca. 1,622 per square mile. The population density for getting a
195 low number of cases at 50% chance is 762 per square mile (Figure 2(c)) , and the arithmetic
196 mean of these two values at high and low cases gives an average of 1,192 per square mile
197 and defined as the population density at which there is a 50% chance of infection. Thus,
198 4.02% (125 of 3,107) of the counties with population density greater than 1,192 per square
199 mile are at 50% or greater risk of infection as on November 30,2020. The key results
200 discussed here are concisely summarized in Table 3.

201

202

203 **Table3:** Key results of Population density- cases analysis

Attribute	Value
Population density beyond which 95% probability of high number of cases	3000 per square mile
Population density beyond which 50% probability of high number of cases	1622 per square mile
Average Population density beyond which 50% probability of getting infected	1192 per square mile
Percentage of US counties at greater than 50% probability of getting infected	4.02%(125 out of 3107)

204

205 Table 4 provides values for population density and arithmetic average probability of high
206 number of cases for each state in the US, as of November 30, 2020.

207

208

209
210
211
212
213
214
215
216
217
218

Table 4: Probabilities of high number of COVID19 cases as of November 30, 2020

State	Population density (per square mile)	Average probability of high cases (Ap)	Maximum probability of high cases (Map)	Minimum probability of high cases (Minp)	Rank of Ap	Rank of Map	Percent difference between Map and Ap
District of Columbia	11569.7	1	1	1.000	1	1	0
New Jersey	1207.8	0.404	1	0.027	2	1	60
Rhode Island	1024.5	0.28	0.652	0.043	3	23	57
Massachusetts	883.5	0.242	1	0.022	4	1	76
Connecticut	736.6	0.156	0.421	0.028	7	27	63
Maryland	622.9	0.165	1	0.019	6	1	84
Delaware	499.6	0.144	0.368	0.030	8	29	61
New York	412.8	0.099	1	0.017	11	1	90
Florida	400.7	0.078	0.981	0.018	13	14	92
Pennsylvania	286.1	0.079	1	0.018	12	1	92
Ohio	286.1	0.066	0.927	0.019	14	18	93

California	253.7	0.12	1	0.017	10	1	88
Illinois	228.2	0.047	0.999	0.018	18	10	95
Hawaii	220.3	0.121	0.52	0.018	9	26	77
Virginia	216.1	0.232	1	0.018	5	1	77
North Carolina	215.7	0.041	0.711	0.018	20	20	94
Indiana	187.9	0.038	0.857	0.018	24	19	96
Georgia	184.6	0.051	0.93	0.018	15	17	95
Michigan	176.7	0.048	0.944	0.018	17	16	95
South Carolina	171.2	0.027	0.077	0.018	32	35	65
Tennessee	165.6	0.031	0.346	0.018	28	30	91
New Hampshire	151.9	0.029	0.053	0.018	31	39	45
Washington	114.6	0.03	0.181	0.017	30	33	83
Kentucky	113.1	0.031	0.706	0.018	28	21	96
Texas	111	0.036	0.952	0.017	27	15	96
Louisiana	107.6	0.04	0.689	0.018	22	22	94
Wisconsin	107.5	0.038	0.993	0.018	24	12	96
Alabama	96.8	0.022	0.071	0.018	37	36	69
Missouri	89.3	0.037	0.999	0.018	26	10	96
West Virginia	74.6	0.023	0.046	0.018	35	42	50
Minnesota	70.8	0.043	0.984	0.017	19	13	96
Vermont	67.7	0.021	0.036	0.018	39	46	42
Arizona	64.1	0.021	0.053	0.018	39	39	60
Mississippi	63.4	0.02	0.042	0.017	42	44	52
Arkansas	58	0.02	0.059	0.018	42	38	66
Oklahoma	57.7	0.025	0.225	0.017	33	32	89
Iowa	56.5	0.021	0.118	0.018	39	34	82
Colorado	55.6	0.049	1	0.017	16	1	95
Oregon	43.9	0.039	0.637	0.017	23	24	94
Maine	43.6	0.022	0.038	0.018	37	45	42

Utah	39	0.041	0.414	0.017	20	28	90
Kansas	35.6	0.023	0.272	0.017	35	31	92
Nevada	28.1	0.02	0.043	0.017	42	43	53
Nebraska	25.2	0.025	0.527	0.017	33	25	95
Idaho	21.6	0.019	0.048	0.017	46	41	60
New Mexico	17.3	0.02	0.069	0.017	42	37	71
South Dakota	11.7	0.018	0.03	0.017	47	47	40
North Dakota	11	0.018	0.022	0.017	47	48	18
Montana	7.3	0.018	0.02	0.017	47	49	10
Wyoming	6	0.018	0.019	0.017	47	50	5

219

220 This average probability is the simple arithmetic average of the respective probabilities of
 221 state counties. It is intuitive that the most densely populated states were also those with the
 222 highest probability of a high number of cases, strengthening the finding that population
 223 density is critical beyond a specific threshold. The average probability for a high number of
 224 COVID-19 cases provides a number useful for conceptualizing the overall risk of infection in
 225 a particular state. However, except for a few densely populated states, epicenter counties are
 226 not highlighted. For example, on November 30, 2020, Texas, California, Florida, and Illinois
 227 were States with the largest number of COVID-19 cases. From Table 4, it was obvious that
 228 the relatively low values of average probabilities for those four states do not reflect their
 229 epicenter status. Therefore, we defined the maximum average probability for a state which is
 230 taken equal to the maximum value of average probabilities considering all the counties of a
 231 state. Thus, the maximum average probability for each state as calculated. The high
 232 probability of a high number of cases (>90%) indicated this metric performed acceptably to
 233 rank a state as an epicenter. Exceptions were noted, where relatively low value of maximum
 234 average probability of high cases was observed in low population density states having high
 235 number of COVID-19 cases. This anomaly is a potential limitation of the logistical regression

236 methods, in dealing with locations with low population densities and high cases. However, it
237 is understood that any regressive model considering population density as the single
238 explanatory variable likely would fail to explain a high number of cases in less densely
239 populated regions. Lastly, an important observation with reference to population density and
240 case analysis can be discerned from Table 4, namely the percentage difference between the
241 maximum and average probabilities of high number of cases, being very high for many states,
242 notably those with high maximum average probabilities. This signifies that only a few
243 counties of the state account for a large number of cases, and the state as a whole would not
244 be an epicenter of COVID-19.

245

246 The analysis in our study assumes a uniform population distribution. In reality, the population
247 is generally not distributed evenly across the county, as most of the population clusters in and
248 around cities. The lack of a standard sub-county level case count, which rules out the
249 possibility of conducting a more realistic city-level threshold analysis, forms a limitation of
250 our study. Furthermore, though county population density is generally considered a reliable
251 predictor to explain COVID-19 cases due to its high explanatory power (Riley, 2007; Wong
252 & Li, 2020) , controlling it for other variables such as population size could bring valuable
253 insights. to determine running thresholds on population density.

254

255 **4. Conclusions and Implications on Future of urban cities**

256 The interrelationship of population density with the number of COVID-19 cases was
257 analyzed, with the objective to determine thresholds for population density above which there
258 was a 50% or greater risk of COVID-19 cases in humans. Population density and COVID-19
259 cases, when analyzed together, suggest *ca.* 4% of the counties (shown in Figure 4) in the

260 United States would be at 50% or greater at risk of COVID-19 cases and confined to a few
261 counties.

262

263

264 The thresholds provide useful information as a guide for policymakers. In combination with
265 other governing factors, the population density threshold can provide a more decisive
266 conclusion, notably for estimating cases and mitigating COVID-19 in human cases,
267 especially for urban neighborhoods that are more likely heterogenous in race, income, and
268 infrastructure (J. A. Maantay, Maroko, & Herrmann, 2007; J. Maantay & Maroko, 2009).
269 Dense populations comprise sub-populations, namely communities of color and low-income
270 communities that are vulnerable, e.g. poor housing, high pollution, lack of access to health
271 care, and a higher rate of pre-existing conditions (Brulle & Pellow, 2006; Bullard, 2005;
272 Pellow, 2000). Nevertheless, the relationship between population density and rates of
273 infection is sufficiently robust that it can be employed by policymakers to prepare
274 anticipatory plans for specific communities and thereby prevent the spread of infection and
275 mitigate the effects of the disease.

276

277 **Data Availability**

278 Raw data sets are publicly available and can be accessed using weblinks provided.

279 Datasets generated in this study are available on openly accessible data servers.

280 <https://github.com/nytimes/covid-19-data>

281 <https://www.census.gov/data/datasets/time-series/demo/popest/2010s-counties-total.html>

282 <https://www.census.gov/library/publications/2011/compendia/usa-counties-2011.html#LND>

283

284 While there are many other links to get the data on COVID-19 case numbers, to the best of
285 our knowledge, GitHub is the only concise yet comprehensive source which provides easy to
286 analyze chronological case count data for US at county scale.

287

288 **Code Availability**

289 All the data analysis was performed using the MINITAB software package, a standard
290 package for statistical analysis available at

291 <https://www.minitab.com/en-us/products/minitab/>

292

293 **References**

294 Atkinson, M., & Wein, L. (2008). Quantifying the Routes of Transmission for Pandemic

295 Influenza. *Bull Math Biol*, 70. <https://doi.org/10.1007/s11538-007-9281-2>

296 Brulle, R. J., & Pellow, D. N. (2006). Environmental justice: Human health and

297 environmental inequalities. *Annual Review of Public Health*, 27(102), 103–124.

298 <https://doi.org/10.1146/annurev.publhealth.27.021405.102124>

299 Bullard, R. (2005). Environmental justice in the 21st century. *Debating the Earth*.

300 Carlson, C. J., Gomez, A. C. R., Bansal, S., & Ryan, S. J. (2020). Misconceptions about

301 weather and seasonality must not misguide COVID-19 response. *Nature*

302 *Communications*, 11(1), 2–5. <https://doi.org/10.1038/s41467-020-18150-z>

303 Chandra, S., Kassens-Noor, E., Kuljanin, G., & Vertalka, J. (2013). A geographic analysis of

304 population density thresholds in the influenza pandemic of 1918-19. *International*

305 *Journal of Health Geographics*, 12, 1–10. <https://doi.org/10.1186/1476-072X-12-9>

306 Cruickshank, R. (1939). Air-borne infection and its prevention. *Public Health*, 53(C), 254–

307 255. [https://doi.org/10.1016/S0033-3506\(39\)80180-9](https://doi.org/10.1016/S0033-3506(39)80180-9)

- 308 Grantz, K. H., Rane, M. S., Salje, H., Glass, G. E., Schachterle, S. E., & Cummings, D. A. T.
309 (2016). Disparities in influenza mortality and transmission related to sociodemographic
310 factors within Chicago in the pandemic of 1918. *National Acad Sciences*, 29, 2020.
311 <https://doi.org/10.5061/dryad.48nv3>
- 312 Hoyle, F., & Wickramasinghe, N. C. (1990). Influenza - evidence against contagion:
313 Discussion paper. *Journal of the Royal Society of Medicine*, 83(4), 258–261.
314 <https://doi.org/10.1177/014107689008300417>
- 315 Li, R., Richmond, P., & Roehner, B. M. (2018). Effect of population density on epidemics.
316 *Physica A: Statistical Mechanics and Its Applications*, 510, 713–724.
317 <https://doi.org/10.1016/j.physa.2018.07.025>
- 318 Maantay, J. A., Maroko, A. R., & Herrmann, C. (2007). Mapping Population Distribution in
319 the Urban Environment: The Cadastral-based Expert Dasymmetric System (CEDS).
320 *Cartography and Geographic Information Science*, 34(2), 77–102.
321 <https://doi.org/10.1559/152304007781002190>
- 322 Maantay, J., & Maroko, A. (2009). Mapping urban risk : Flood hazards , race , &
323 environmental justice in New York. *Applied Geography*, 29(1), 111–124.
324 <https://doi.org/10.1016/j.apgeog.2008.08.002>
- 325 Merler, S., & Ajelli, M. (2010). The role of population heterogeneity and human mobility in
326 the spread of pandemic influenza. *Proceedings of the Royal Society B: Biological*
327 *Sciences*, 277(1681), 557–565. <https://doi.org/10.1098/rspb.2009.1605>
- 328 Merow, C., & Urban, M. C. (2020). Seasonality and uncertainty in global COVID-19 growth
329 rates. *Proceedings of the National Academy of Sciences of the United States of America*,
330 117(44), 27456–27464. <https://doi.org/10.1073/pnas.2008590117>

- 331 Pellow, D. N. (2000). Environmental Inequality Formation. *American Behavioral Scientist*,
332 43(4), 581–601. <https://doi.org/10.1177/0002764200043004004>
- 333 Pequeno, P., Mendel, B., Rosa, C., Bosholn, M., Souza, J. L., Baccaro, F., ... Magnusson, W.
334 (2020). Air transportation, population density and temperature predict the spread of
335 COVID-19 in Brazil. *PeerJ*, 8, e9322. <https://doi.org/10.7717/peerj.9322>
- 336 Riley, S. (2007). Large-Scale Spatial-Transmission Models of Infectious Disease. *Science*,
337 316(5829), 1298–1301. <https://doi.org/10.1126/science.1134695>
- 338 Robinson, M., Stilianakis, N. I., & Drossinos, Y. (2012). Spatial dynamics of airborne
339 infectious diseases. *Journal of Theoretical Biology*, 297, 116–126.
340 <https://doi.org/10.1016/j.jtbi.2011.12.015>
- 341 Wong, D. W. S., & Li, Y. (2020). Spreading of COVID-19: Density matters. *PLOS ONE*,
342 15(12), e0242398. <https://doi.org/10.1371/journal.pone.0242398>
- 343 WHO Coronavirus (COVID-19) Dashboard. (2021). Retrieved April 28, 2021, from
344 <https://covid19.who.int/>
345
346
347
348
349
350
351
- 352 **References from the Supplementary section**
- 353 Hosmer, D. W., & Lemeshow, S. (2000). *Applied Logistic Regression (Wiley Series in*
354 *Probability and Statistics)* (2nd ed.). <https://doi.org/10.1002/0471722146>

355 Methods and formulas for Ordinal Logistic Regression - Minitab. (2019). Retrieved October
356 19, 2020, from [https://support.minitab.com/en-us/minitab/18/help-and-how-](https://support.minitab.com/en-us/minitab/18/help-and-how-to/modeling-statistics/regression/how-to/ordinal-logistic-regression/methods-and-formulas/methods-and-formulas/#measures-of-association)
357 [to/modeling-statistics/regression/how-to/ordinal-logistic-regression/methods-and-](https://support.minitab.com/en-us/minitab/18/help-and-how-to/modeling-statistics/regression/how-to/ordinal-logistic-regression/methods-and-formulas/methods-and-formulas/#measures-of-association)
358 [formulas/methods-and-formulas/#measures-of-association](https://support.minitab.com/en-us/minitab/18/help-and-how-to/modeling-statistics/regression/how-to/ordinal-logistic-regression/methods-and-formulas/methods-and-formulas/#measures-of-association).

359

360

361

362

363

364

365 **Author Contributions**

366 A.J. is responsible for the main concepts; Y.J. and M.G. wrote the study; Y.J., M.G., M.U.
367 and A.J. carried out the analyses; C.Y.W., T.N. A.A. and R.C. prepared the final
368 manuscript.

369

370 **Corresponding author**

371 Antarpreet Jutla

372

373 **Competing interests**

374 The authors declare no competing interests.

375

376

377

378

379

380

381

382

383

384 **List of figures**

385 Figure 1: Performance of logistical regression model on a biweekly scale for the entire US.

386 Figure 2: Average infection probability versus population density for (a) high (b) medium
387 and (c) low number of cases

388 Figure 3. Plots show changes in the probability of (a) high (b)medium and (c) low number of
389 cases.

390
391 Figure 4: US counties with greater than, and less than 50% probability of COVID-19
392 infection as of November 30 ,2020.

393
394
395

396

397

398 **List of tables**

399 Table 1: Biweekly 80th percentile cases

400 Table 2: Variation in log likelihood for COVID-19 cases (November 30,2020)

401 Table 3: Key results of Population density- cases analysis

402 Table 4: Probabilities for high number of COVID19 cases (as on November 30,2020)

403 Table S1: Results from the ordinal logistic regression model (November 15,2020)

404

405

406

407

408

409

410

411

412

413

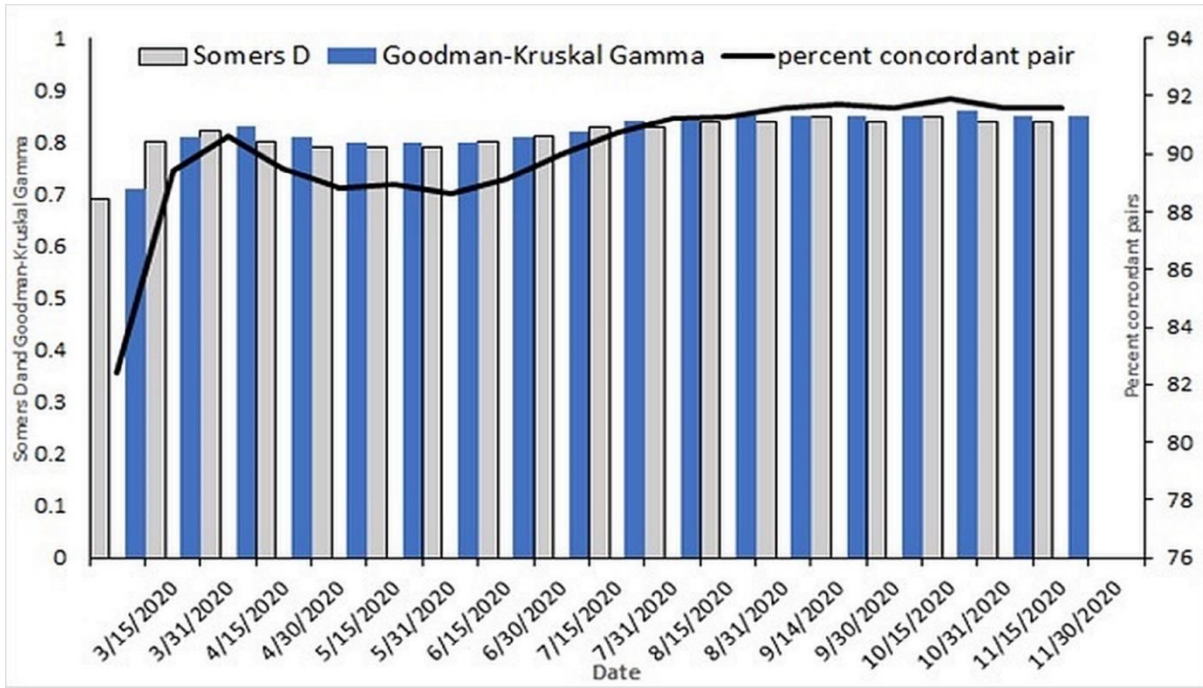
414

415

416 **Figures:**

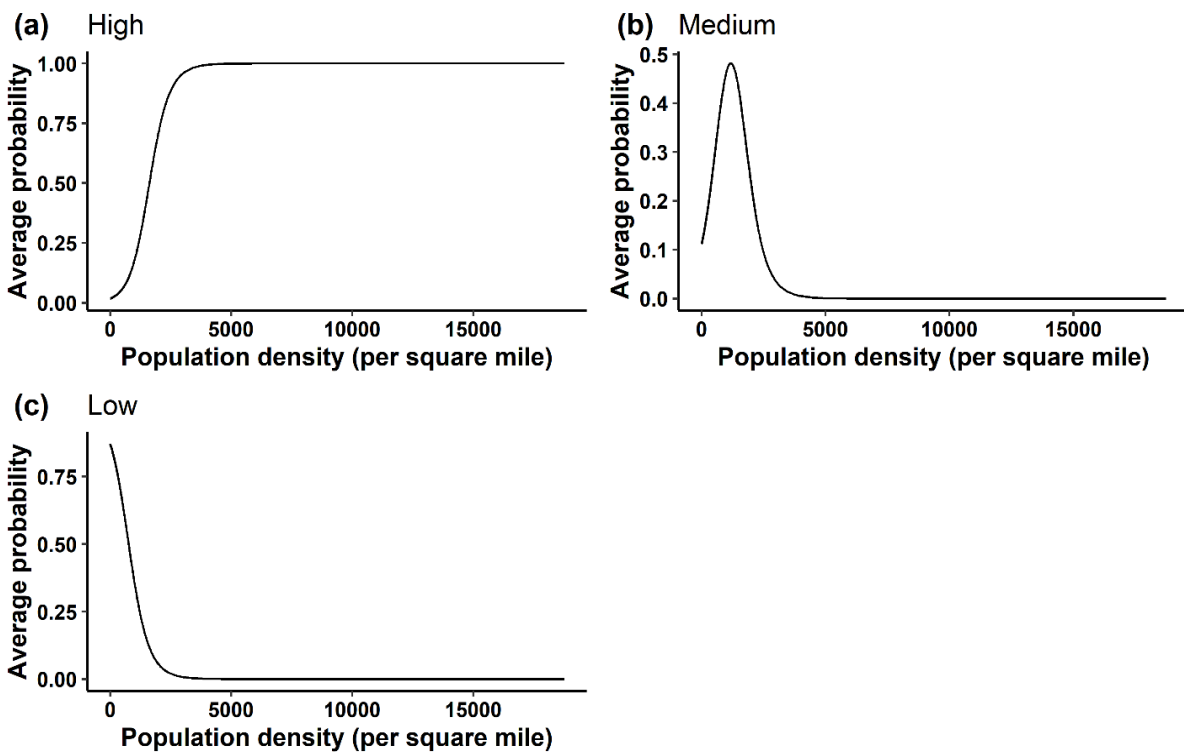
417

418



419
420
421
422
423

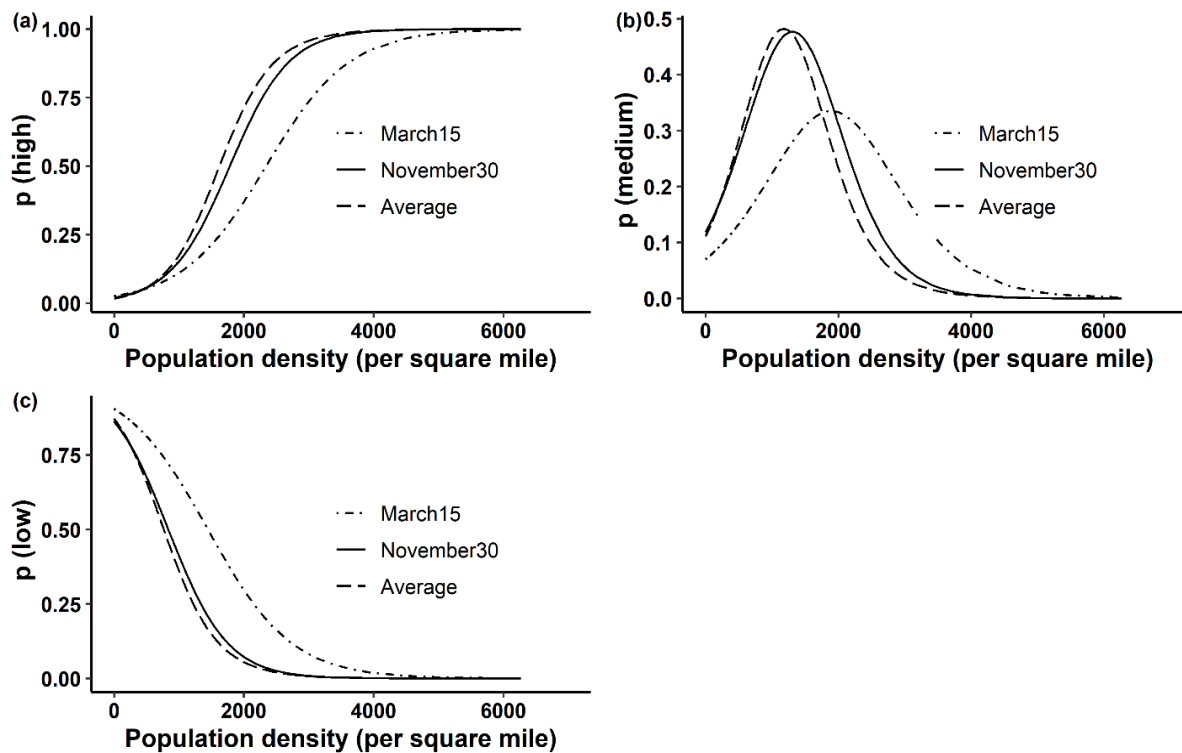
Figure 1: Performance of logistical regression model on a biweekly scale for the entire USA



424
425

426 **Figure 2:** Average probability vs population density for (a) High (b) Medium (c) Low
427 number of cases, from March 15, 2020, to November 30, 2020

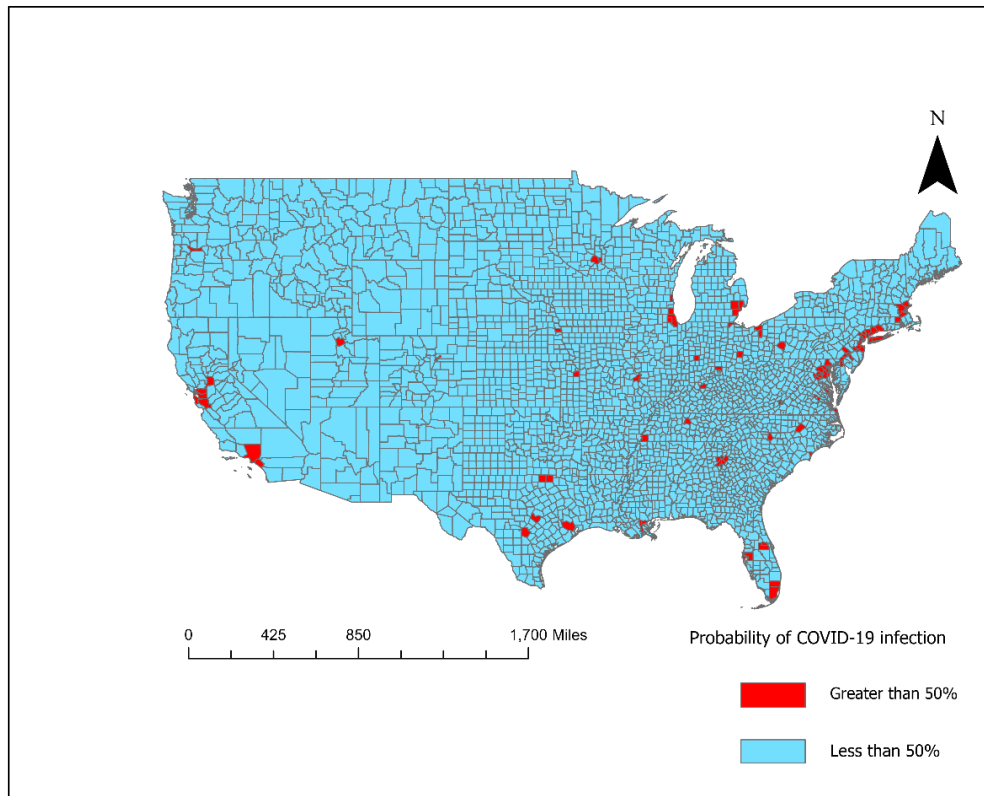
428



429

430 **Figure 3.** Changes in bi-weekly probability from March 15, 2020, to November 30, 2020 of
431 (a) high , (b) medium, and (c) low number of cases

432



433

434 **Figure 4:** US counties with greater than 50% probability of getting infected as of November
435 30,2020.

436

437